Journal of Power Sources 249 (2014) 392–396

Contents lists available at ScienceDirect

Journal of Power Sources

journal homepage: www.elsevier.com/locate/jpowsour

Short communication

Preparation and electrochemical properties of gel polymer electrolytes using triethylene glycol diacetate-2-propenoic acid butyl ester copolymer for high energy density lithium-ion batteries

Huanhuan Fan [a], Hongxiao Li [a], Li-Zhen Fan [a,*], Qiao Shi [b]

[a] Institute of Advanced Materials and Technology, University of Science and Technology Beijing, Beijing 100083, China
[b] Shenzhen Capchem Technology Co., Ltd., Shenzhen 518118, China

HIGHLIGHTS

- BA–TEGDA copolymer-based GPE were prepared by in situ thermal polymerization.
- The GPE had a well cross-linked framework and excellent mechanical properties.
- The in situ polymerization simplified the assembly process of batteries greatly.
- The GPE could satisfy the use of the high-voltage positive electrode material.

ARTICLE INFO

Article history:
Received 24 September 2013
Received in revised form
19 October 2013
Accepted 24 October 2013
Available online 6 November 2013

Keywords:
Gel polymer electrolyte
Ionic conductivity
In situ polymerization
Lithium-ion batteries

ABSTRACT

Gel polymer electrolytes (GPE) composed of triethylene glycol diacetate (TEGDA)–2-propenoic acid butyl ester (BA) copolymer and commercial used liquid organic electrolyte are prepared via in situ polymerization. The ionic conductivity of the as-prepared GPE can reach 5.5×10^{-3} S cm^{-1} with 6 wt% monomers and 94 wt% liquid electrolyte at 25 °C. Additionally, the temperature dependence of the ionic conductivity is consistent with an Arrhenius temperature behavior in a temperature range of 20–90 °C. Furthermore, the electrochemical stability window of the GPE is 5 V at 25 °C. A Li|GPE|(Li[$Li_{1/6}Ni_{1/4}Mn_{7/12}$]$O_2$) cell has been fabricated, which shows good charge–discharge properties and stable cycle performance compared to liquid electrolyte under the same test conditions.

1. Introduction

Gel polymer electrolytes (GPE) have received increasing interest worldwide since they overcame the safety problems caused by liquid electrolyte such as the possibility of leakage [1,2]. Furthermore, due to the easily shaped properties, the gel polymer electrolytes permit the development of thin batteries with design flexibility. Nowadays, considerable efforts are being focused on the development of new types of advanced lithium-ion batteries with GPE. In order to provide high power density, GPE should have good mechanical properties, stable performance in the practical applications and high ionic conductivity at ambient temperature [3]. Since the first demonstration of GPE reported by Feullade and Perche in 1975 [4], various polymers such as poly(acrylonitrile) (PAN) [5,6], poly(vinylidene fluoride) (PVDF) [7,8], poly(methyl methacrylate) (PMMA) [9,10], poly(vinyl chloride) (PVC) [11,12], poly(ethylene oxide) (PEO) [13,14] and poly(vinylidene fluoride-co-hexafluoropropylene) (PVdF-HFP) [15,16] have been widely used as polymer matrices for the preparation of GPE. In the GPE, the liquid electrolytes are retained in a polymer framework and contribute to the ionic conduction, whereas the host polymer provides dimensional stability to the gel electrolyte system. The most advantageous features of these electrolytes lie in their free-standing consistency and high ionic conductivities exceeding 10^{-4} S cm^{-1}, which is significant for battery applications.

It is critical to develop suitable GPE with good lithium interface stability, high electrochemical stability, high mechanical strength and high ionic conductivity for lithium ion batteries. As a common matrix polymer used in the GPE, PMMA has been proposed for lithium battery applications [17]. Meanwhile, its amorphous

* Corresponding author. Tel./fax: +86 10 62334311.
E-mail addresses: fanlizhen@ustb.edu.cn, fanlizhen@gmail.com (L.-Z. Fan).

0378-7753/$ – see front matter © 2013 Elsevier B.V. All rights reserved.
http://dx.doi.org/10.1016/j.jpowsour.2013.10.112

structure is beneficial to the ionic conduction (1×10^{-3} S cm^{-1} at ambient temperature). Besides, the PMMA-based gel electrolytes have exhibited excellent interfacial stability towards lithium metals. It has also been reported that gel electrolytes based on cross-linked PMMA can suppress the formation of lithium dendrite [18]. In order to form free-standing films with a high content of organic solvents, however, PMMA has to be blended with other polymers such as poly(vinyl chloride) (PVC) [19] and acrylonitrile–butadiene–styrene terpolymer (ABS) [20]. Besides, the GPE can be prepared by ultraviolet-curing (UV), solvent-casting techniques, phase-inversion methods and in situ polymerization. Particularly, in the case of in situ polymerization, the preparation of the electrolyte membrane and the assembly of the batteries could be achieved in one step, effectively improving the production efficiency and reducing the costs [21,22]. A precursor consisted of a curable monomer and a liquid electrolyte was directly put into the lithium ion battery cell, followed by curing to form a polymer network [23]. Due to the relatively low viscosity, the precursor can be easily wetted into the electrodes and separators, then resulting in good contact and affinity with the electrode and electrolytes.

In this work, in order to prepare highly conductive GPE with high mechanical strength, TEGDA–BA copolymer has been synthesized as the polymer matrix for the GPE,2,2′-Azobis-(2,4-dimethylvaleronitrile) (ABVN) as the thermal initiator, and 1 M $LiPF_6$/ethylene carbonate (EC):dimethylcarbonate (DMC):ethylmethylcarbonate (EMC) (1:1:1 in volume) as the electrolyte. By using in situ polymerization, the precursor was directly put into the lithium ion battery cell, followed by curing to form a polymer network. The two vinyl bonds at the end of TEGDA can form a dense network structure, which leads to high mechanical strength for the polymer. The ionic conductivities and electrochemical properties of the GPE were examined. A high capacity cathode material ($Li[Li_{1/6}Ni_{1/4}Mn_{7/12}]O_2$) has been prepared to assemble the Li|GPE|($Li[Li_{1/6}Ni_{1/4}Mn_{7/12}]O_2$) cells and the electrochemical characteristics and cycling performance were evaluated.

2. Experimental

To synthesize the GPE, TEGDA and BA (CAPCHEM CO., LTD.) were prepared as the monomer mixtures in a weight ratio of 2:4. An appropriate amount of ABVN (CAPCHEM CO., LTD.) (1 wt% the monomer mixtures) was added as thermal initiator. A battery grade solution of 1 M LiPF6/EC:DMC:EMC (1:1:1 in volume) (CAPCHEM CO., LTD.)was added and then the solution was further stirred. The amount of electrolyte solution (94 wt%) was added based on the total weight of the GPE composed of matrix polymer and liquid electrolyte. All the procedures were carried out in the glove box with argon gas. The GPE was synthesized after keeping the precursor in a water bath at 80 °C (30 min) for thermal polymerization.

The cross section morphology of the GPE membrane was observed by a scanning electron microscopy (SEM) on an EVO 18 system. Pore diameters of these membranes and their distribution were estimated based on SEM micrographs. Mechanical stress versus strain measurement of electrolyte was performed by applying stress with a compression speed of 0.5 mm min^{-1} using a circular electrolyte plate with the diameter of 20 mm and the thickness of 1 mm on a WDS-5 electronic universal testing machine (Changchun Chao yang test instrument Co. LTD).

The GPE was sandwiched between two platinum electrodes to fabricate the testing cell for ionic conductivity measurement. The AC impedance measurement was performed using a CHI660C impedance analyzer over the frequency range from 10^5 Hz to 1 Hz with the potential amplitude of 5 mV. In order to investigate the temperature dependence of ionic conductivity for GPE, the measurement was carried out in the range of 20–90 °C.

The electrochemical stability window of the GPE was measured by cyclic voltammetry at room temperature using stainless steel as the working electrode and lithium as both the counter and reference electrodes. Electrochemical stability was scanned in a potential range of −0.5 to 5 V versus Li/Li$^+$ at a scanning rate of 1 mV s^{-1}.

The lithium nickel manganese oxide ($Li[Li_{1/6}Ni_{1/4}Mn_{7/12}]O_2$) cathode was coated on an aluminum foil consisted of 80 wt% active material oxide, 15 wt% acetylene black and 5 wt% PVDF. $Li[Li_{1/6}Ni_{1/4}Mn_{7/12}]O_2$ cathode active material was synthesized by the co-precipitation method followed by a high-temperature solid-state reaction. A carbonate precursor $Ni_{0.3}Mn_{0.7}CO_3$ was firstly prepared by the coprecipitation of a 2 mol L^{-1} aqueous solution of Ni, Mn sulfate (Ni:Mn = 3:7 in molar) and a 2 mol L^{-1} solution of Na_2CO_3 with 0.3 M NH_4OH added as a chelating agent. The pH of the mixed solution was adjusted to 8 and the co-precipitation temperature was controlled at 55 °C. The obtained $Ni_{0.3}Mn_{0.7}CO_3$ was washed with deionized water several times and subsequently dried in a vacuum oven. Thereafter the carbonate $Ni_{0.3}Mn_{0.7}CO_3$ was thoroughly mixed with Li_2CO_3 according to the stoichiometric ratio, and then annealed in air at 450 °C for 6 h to decompose the carbonate precursors followed by calcining at 850 °C for 10 h. The Li foil was used as anode and Celgard 2400 as the separator. A 2032 type of coin cell was fabricated in the glove-box filled with argon gas. In the fabrication process, the precursor, the blend of 6 wt% monomer mixtures, 1 wt% initiator, and 94 wt% liquid electrolyte, was added into the assembled cell. The assembled cells were settled for 4 h to ensure the precursor solution to be well wetted into the electrodes and then the cell was heated at the temperature of 80 °C (30 min) for polymerization. The charge and discharge cycling tests of the lithium-ion polymer cells were conducted at 25 °C, and the voltage range of the Li|GPE|($Li[Li_{1/6}Ni_{1/4}Mn_{7/12}]O_2$) cell was2.0–4.8 V. For the comparison, the conventional battery with liquid electrolyte instead of precursor solution of GPE was also assembled, and tested under the same conditions.

3. Results and discussion

The GPE were prepared via the in situ polymerization by copolymerizing the monomers TEGDA and BA. As shown in Scheme 1, the primary radicals were firstly formed by the decomposition of the initiator, which open the double bonds of the vinyl monomers to form a monomer radical. Then, the monomer radicals continue to open the double bond of the other vinyl monomers for the addition reaction. After that, the polymer molecular chains gradually increase with the addition of the vinyl monomer chain, and ultimately formed a three-dimensional structure of the polymer backbone. It is well-known that both the industrial assembling method and practical application safety, mechanical properties are key factors [24]. The stress–strain curve of GPE is shown in Fig. 1a.

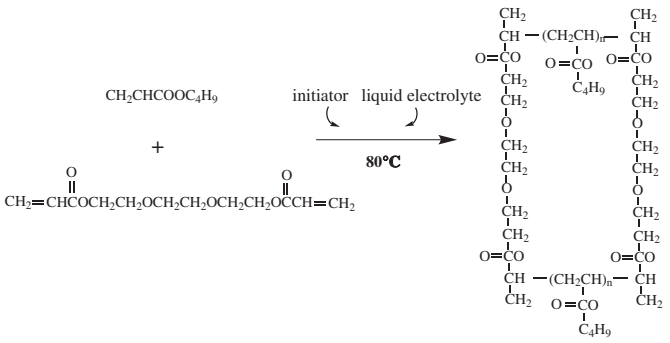

Scheme 1. Synthesis of the copolymer of 2-propenoic acid butyl ester (BA) and triethylene glycol diacetate (TEGDA).

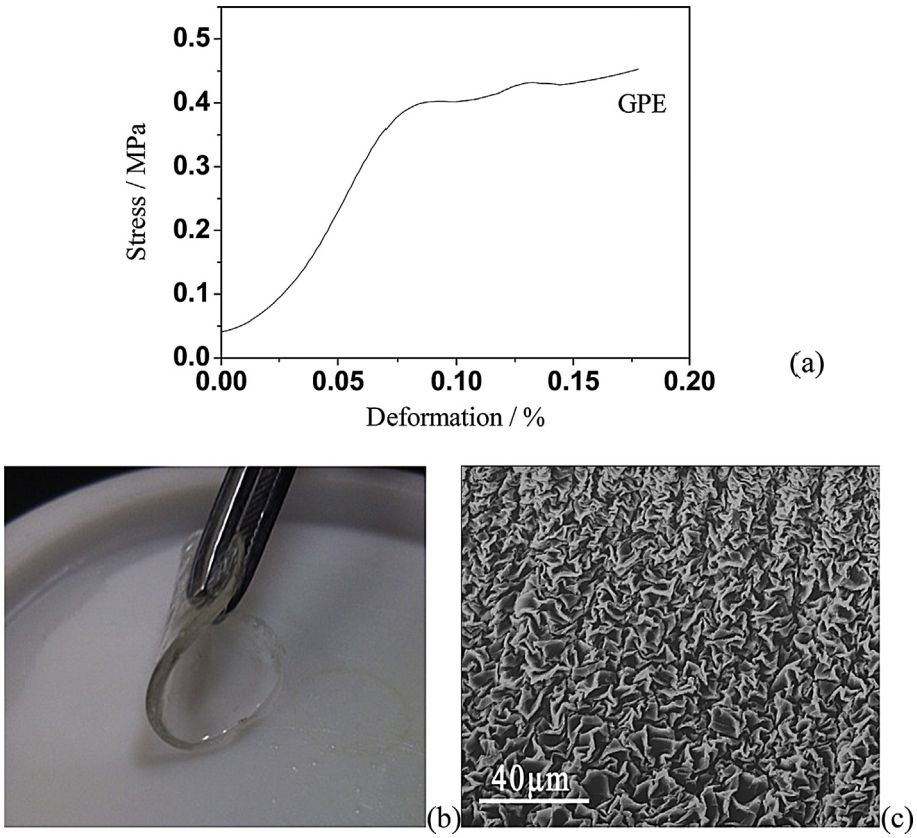

Fig. 1. Stress–strain curve of gel polymer electrolytes membranes (a); photo of self-standing film (b) and SEM image (c) of BA–TEGDA copolymer-based GPE membrane.

The maximum stress of the GPE membrane is 0.45 MPa. Besides, as shown in Fig. 1b, the polymer membranes exhibit excellent dimensional stability, mechanical strength and elasticity when the precursor was constituted by 6 wt% monomer mixtures, 1 wt% initiator, and 94 wt% liquid electrolyte. Herein, our results indicate that even at the low polymer content, the resulting conducting films were still robust, self-standing and flexible with no liquid flow, which is sufficient for practical applications. Moreover, the synthesis technique via in situ polymerization allows precise control and variation of the composition for the electrolyte membranes to optimize electrochemical and mechanical properties.

SEM micrograph (Fig. 1c) of the GPE film was obtained to observe the three-dimensional network structure of the polymer matrix. It is observed that the polymer matrix shows porous structure at microscopic level. In the GPE, it is worth noting that the liquid electrolyte is well dispersed in the polymer matrix. Due to presence of large number of the liquid electrolyte, the porous structure not only provides good mechanical strength, but ensures the high conductivity for the GPE at room temperature.

The ionic conductivities are calculated by Equation (1):

$$\sigma = \frac{d}{SR_b} \tag{1}$$

where d is the electrolyte thickness (cm), S the activity area (cm^2), and R_b the resistance of the electrolyte (Ω). Fig. 2 shows the temperature dependence (in the range of 20–90 °C) of ionic conductivities of GPE and liquid electrolyte. Two smooth curves with linear enhancement were obtained. It can be seen that the liquid electrolyte presents higher ionic conductivities than GPE. Both of the conductivities show Arrhenius temperature behavior, i.e., the ionic conductivity increased with increasing temperature. The ionic conductivities are on the order of magnitude of 10^{-3} S cm^{-1} in the investigate temperature range, and the difference of ionic conductivity at 25 °C between the GPE 5.5 × 10^{-3} S cm^{-1} and the liquid electrolyte 8.3 × 10^{-3} S cm^{-1} is very slight. Besides, the conductivity curve of the GPE exhibited similar variation trend to that of liquid electrolyte, indicating major contribution of liquid electrolyte in the GPE. Furthermore, the temperature-dependence conductivity of the GPE can be explained by the free-volume model [25]. As temperature increases, the migration of carrier ions could be improved and, on the other hand, the polymer could be expanded. The expansion could produce local vacancies and increase the free volume, consequently promoting the motion of the ions and polymer segments. Thus, the ions, solvated molecules and polymer segments could easily travel into the free volume to enhance the ionic conductivities [26].

The compatibility of the GPE with lithium metals has been evaluated by analyzing the impedance variation of the Li|GPE|Li cells for a period of 3 days. Fig. 3 shows a semi-circle impedance

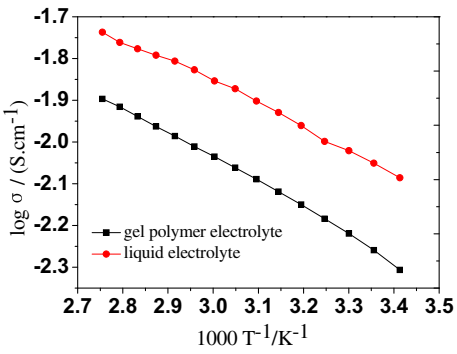

Fig. 2. Ionic conductivities of GPE and 1 M $LiPF_6$/EC:DMC:EMC liquid electrolyte at various temperatures.

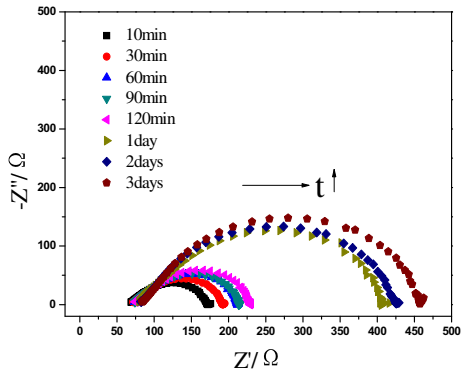

Fig. 3. AC impedance spectra of Li|GPE|Li cell tested at different time.

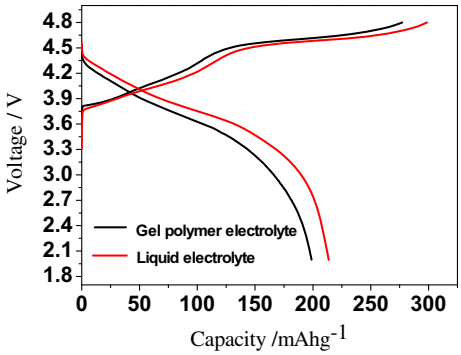

Fig. 5. Initial charge–discharge curves of Li|GPE|(Li[$Li_{1/6}Ni_{1/4}Mn_{7/12}$]$O_2$) and Li|1 M $LiPF_6$/EC:DMC:EMC|(Li[$Li_{1/6}Ni_{1/4}Mn_{7/12}$]$O_2$) cells at 0.2 C.

spectrum for this cell, which is typical contribution from the bulk electrolyte resistance (R_b) and electrode/electrolyte interfacial resistance (R_f). After 3 days, the variation of the interfacial resistance (R_f) was found to increase compared to the beginning, with the resistance value changed from 170 Ω to 460 Ω. Moreover, the compatibility of the GPE with lithium metals also showed relatively good interfacial stability. The increase of R_f during the storage seems to be associated with the growth of a solid–electrolyte interface layer (SEI) and a passivation layer on the lithium electrode surface [27].The trace amount of water in the electrolyte will result in the formation of HF by reacting with $LiPF_6$. Also a LiF layer can be formed on the surface of the lithium electrode due to the high reactivity of HF, which would lead to the increased interfacial resistance (R_f) [28,29]. Besides, the degradation of the physical contact between the electrolyte and lithium electrode could also lead to the growth of the SEI layer, and then cause an increase of interfacial resistance (R_f).

Electrochemical stability and lithium plating/stripping characteristics were studied by measuring cyclic voltammetry of the GPE using a Li|GPE|Stainless Steel cell. Cyclic voltammograms of the GPE measured between −0.5 and 5.0 V *vs.* Li/Li^+ are presented in Fig. 4. There were no significant oxidation or reduction peaks in the reversible plating and stripping of lithium except at potential range of −0.5 to 0.5 V. This suggests that there was no oxidative degradation of the GPE in this voltage range and a wide electrochemical stability window was obtained which would be sufficient for application in rechargeable lithium ion batteries. Besides, the peak current of the voltammogram is relatively high and the peak areas are similar, indicating that the process of the lithium plating/stripping is reversible and the efficiency is high.

A Li|GPE|(Li[$Li_{1/6}Ni_{1/4}Mn_{7/12}$]$O_2$) cell was fabricated in order to evaluate the electrochemical performance of a lithium-ion polymer cell using the GPE. The assembled cell was pre-conditioned with a cut-off voltage of 4.8 V as the upper limit and 2.0 V as the lower limit at 0.2 C. Fig. 5 displays two charge–discharge curves of the cell at the constant current density. One of them is the pure liquid electrolyte cell used as a comparison with the GPE battery. No obvious difference was observed between the two charge–discharge curves, and the first discharge capacity are 213 mAh g^{-1} and 199 mAh g^{-1} for the pure liquid electrolyte cell and GPE battery, respectively, demonstrating that the GPE can still maintain a high discharge capacity during the first cycle. Besides, an irreversible capacity loss could be observed on the first charge–discharge process for both of them, which is owing to the formation of passivation film on the surface of the Li electrode caused by the decomposition of the electrolyte during the initial cycling. The passivation film can prevent the electrolyte from further reduction by the active lithium and thus limiting the degradation of electrolytes.

The discharge capacities as a function of cycle number for the cells prepared with the liquid electrolyte and the GPE are illustrated in Fig. 6. It can be seen that the cell with GPE shows a very stable discharge capacity during charge–discharge cycling. The discharge capacity shows no obvious capacity decline during the 50 cycles. The good cycling characteristic of the cell can be attributed to the effective ionic transport between electrodes and good compatibility between the electrolyte and electrode, especially with lithium metal. This also demonstrates that the GPE membranes are promising for lithium-ion battery applications. The decline in the capacity is primarily due to the loss of interfacial contact between the electrodes and the GPE upon cycling [30], which would increase the internal resistance of the cell. Furthermore, a cross-linking reaction causes an increase in the resistance for ion migration in both the electrolyte and the electrodes, resulting in a decrease in the

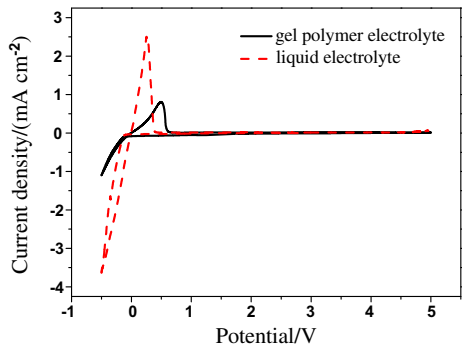

Fig. 4. Cyclic voltammograms of the GPE and 1 M $LiPF_6$/EC:DMC:EMC liquid electrolyte on SS work electrode at a scan rate of 1 mV s^{-1}.

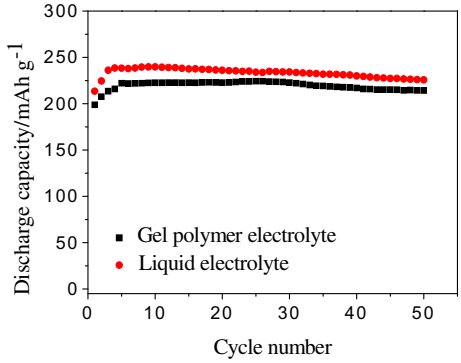

Fig. 6. Discharge capacities of Li|GPE|(Li[$Li_{1/6}Ni_{1/4}Mn_{7/12}$]$O_2$) and Li|1 M $LiPF_6$/EC:DMC:EMC|(Li[$Li_{1/6}Ni_{1/4}Mn_{7/12}$]$O_2$) cells as a function of cycle number.

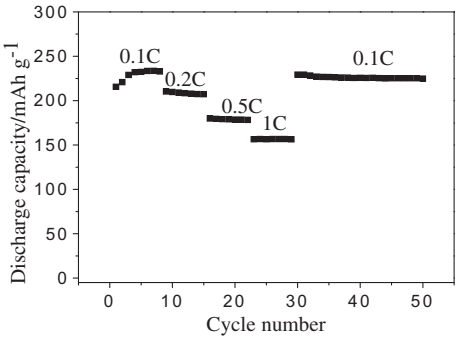

Fig. 7. Cycle performance and rate capabilities of Li|GPE|(Li[$Li_{1/6}Ni_{1/4}Mn_{7/12}$]$O_2$) cell.

discharge capacity. Fig. 7 shows the discharge capacity curves obtained at different current densities. The cell delivers a discharge capacity of 226 mAh g^{-1} at 0.1 C, and 157 mAh g^{-1} at a 1 C, which is 69% of the discharge capacity at 0.1 C. The battery operated with the expected voltage profiles delivers a good fraction of the theoretical capacity even at 1 C.

4. Conclusions

The GPE consisted of 1 M $LiPF_6$/EC:DMC:EMC (1:1:1 in Volume) and TEGDA–BA copolymer was synthesized via in situ polymerization, and exhibited high ionic conductivity around 5.5×10^{-3} S cm^{-1} at 25 °C and good electrochemical stability up to 5 V *vs.* Li/Li^+. A stable R_f value was detected on the interface of GPE and lithium metal. It has also been found that the GPE membranes are freestanding, highly homogeneous and elastic, simultaneously, with excellent mechanical integrity and strength. The first discharge capacity of 199 mAh g^{-1} of the Li|GPE|(Li[$Li_{1/6}Ni_{1/4}Mn_{7/12}$]$O_2$) cell was observed at 0.2 C. Besides, the discharge capacity of the cell with GPE remained stable during charge–discharge cycling. Apparently, the novel GPE prepared by in situ method is anticipated to be a potential candidate for applications in high energy density lithium-ion batteries with high ionic conductivity, high electrochemical window, and good compatibility with the electrodes.

Acknowledgments

This work was supported by the 973 Project (2013CB934001), NSF of China (51172024, 51372022) and Fundamental Research Funds for the Central Universities of China (FRF-TP-09-007A).

References

[1] B. Scrosati, J. Garche, J. Power Sources 195 (2010) 2419.
[2] P. Raghavan, X. Zhao, J.K. Kim, J. Manuel, G.S. Chauhan, J.H. Ahn, C. Nah, Electrochim. Acta 54 (2008) 228.
[3] J.M. Tarascon, M. Armand, Nature 414 (2001) 359.
[4] G. Feullade, P. Perche, J. Appl. Electrochem. 5 (1975) 63.
[5] Y.H. Liang, C.C. Wang, C.Y. Chen, J. Power Sources 176 (2008) 340.
[6] A.I. Gopalan, P. Santhosh, K.M. Manesh, J.H. Nho, S.H. Kim, C.G. Hwang, K.P. Lee, J. Membr. Sci. 325 (2008) 683.
[7] M.S. Park, S.H. Hyun, S.C. Nam, S.B. Cho, Electrochim. Acta 53 (2008) 5523.
[8] M. Stolarska, L. Niedzicki, R. Borkowska, A. Zalewska, W. Wieczorek, Electrochim. Acta 53 (2007) 1512.
[9] J.P. Sharma, S.S. Sekhon, Solid State Ionics 178 (2007) 439.
[10] Y.H. Liao, D.Y. Zhou, M.M. Rao, W.S. Li, Z.P. Cai, Y. Liand, C.L. Tan, J. Power Sources 189 (2009) 139.
[11] S. Rajendran, M.R. Prabhu, M.U. Rani, J. Power Sources 180 (2008) 880.
[12] E.M. Shembel, O.V. Chervakov, L.I. Neduzhko, I.M. Maksyuta, Y.V. Polischuk, D.E. Reisner, P. Novak, D. Meshri, J. Power Sources 96 (2001) 20.
[13] J.W. Choi, G. Cheruvally, Y.H. Kim, J.K. Kim, J. Manuel, P. Raghavan, J.H. Ahn, K.W. Kim, H.J. Ahn, D.S. Choi, C.E. Song, Solid State Ionics 178 (2007) 1235.
[14] A.M. Christie, S.J. Lilley, E. Staunton, Y.G. Andreev, P.G. Bruce, Science 433 (2005) 50.
[15] P. Raghavan, J.W. Choi, J.H. Ahn, G. Cheruvally, G.S. Chauhan, H.J. Ahn, A. Nah, J. Power Sources 184 (2008) 437.
[16] P. Raghavan, X. Zhao, J. Manuel, G.S. Chauhan, J.H. Ahn, H.S. Ryu, H.J. Ahn, K.W. Kim, C. Nah, Electrochim. Acta 55 (2010) 1347.
[17] C.S. Kim, S.M. Oh, J. Power Sources 109 (2002) 98.
[18] T. Tatsuma, M. Taguchi, N. Oyama, Electrochim. Acta 46 (2001) 1201.
[19] N.S. Choi, J.K. Park, Electrochim. Acta 46 (2001) 1453.
[20] X. Hou, K. Siow, Polymer 41 (2000) 8689.
[21] S. Kuwabata, M. Tomiyori, J. Electrochem. Soc. 149 (2002) A988.
[22] H.S. Kim, J.H. Shin, C.H. Doh, S.I. Moon, S.P. Kim, J. Power Sources 112 (2002) 469.
[23] D. Zhou, L.Z. Fan, H.H. Fan, Q. Shi, Electrochim. Acta 89 (2013) 334.
[24] Z. Tian, X.M. He, W.H. Pu, C.R. Wan, C.Y. Jiang, Electrochim. Acta 52 (2006) 688.
[25] S. Rajendran, T. Uma, J. Power Sources 88 (2000) 282.
[26] G.Y. Gu, S. Bouvier, C. Wu, R. Laura, M. Rzeznik, K.M. Abraham, Electrochim. Acta 45 (2000) 3127.
[27] W.L. Qui, X.H. Ma, Q.H. Yang, Y.B. Fu, X.F. Zong, J. Power Sources 138 (2004) 245.
[28] D. Aurbach, E. Zinigrad, Y. Cohen, H. Teller, Solid State Ionics 148 (2002) 405.
[29] L. Larush, E. Zinigrad, Y. Goffer, D. Aurbach, Langmuir 23 (2007) 12910.
[30] D.W. Kim, Y.K. Sun, J. Power Sources 102 (2001) 41.